PROPAGATION OF P-MODES INTO THE SOLAR ATMOSPHERE

Y. Taroyan, R. Erdélyi, and C. Malins

Solar Physics and upper-Atmosphere Research Group, Department of Applied Mathematics, University of Sheffield, Sheffield, S3 7RH, England

ABSTRACT

We present a simple 1D two-layer model for the study of the propagation of p-modes into the solar atmosphere. The wave motion is governed by the Klein-Gordon equation. Analytical expressions for the solutions are derived. Depending on the frequency, the waves can be either propagating or evanescent. The analytical solutions are used to estimate the flow of energy into the solar atmosphere as a function of frequency. The results predicted by the model are compared with the results derived from an empirical model with a VAL atmosphere. We conclude that the presented model could be useful in interpreting the dynamics and energetics of the solar atmosphere.

Key words: p-modes; magnetic flux tubes; solar atmosphere.

1. INTRODUCTION

According to the traditional view, the solar global p-mode oscillations have little effect as far as the the energetics and the dynamics of the solar atmosphere are concerned. However, over the past few years, there have been some significant advances and a sizeable amount of literature has been dedicated to the study of the leakage and propagation of p-modes into the solar atmosphere. Propagating slow magnetoacoustic waves with periods around 5 minutes were detected near the footpoints of coronal loops (Berghmans & Clette 1999; De Moortel et al. 2000). De Pontieu et al. (2005) showed that these waves could be associated with the p-mode oscillations. De Pontieu, et al. (2003) demonstrated that intensity oscillations in the upper transition region above active regions are excited at chromospheric or even photospheric heights and show a correlation with the p-modes. De Pontieu, Erdélyi & James (2003) pointed out that inclined magnetic field lines create favourable conditions for the leakage of the p-modes into the solar atmosphere and the generation of spicules. The observations of Marsh & Walsh (2006) present an additional evidence for the propagation of p-modes into the solar corona along the magnetic field. There have been recent speculations regarding the modulation of the reconnection rate of magnetic field lines by p-modes required for the excitation of explosive events (Chen& Priest 2006). It has been recognised that significant steps forward can be made if the solar interior and atmosphere are treated as part of a single physical system. In the light of the above-mentioned developments, it becomes clear that analytical models are often required for a deeper understanding of the physical processes, which link the waves in the interior to the waves in the atmosphere.

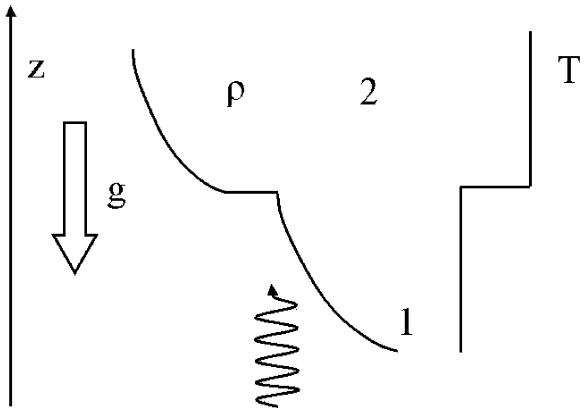

Figure 1. A 1D two-layer model depicting a stratified solar atmosphere. The lower part of the atmosphere (region 1) is separated from the upper part 2 by a density and temperature discontinuity. The waves are launched at $z = 0$ and propagate in the vertical z-direction.

2. MODEL AND GOVERNING EQUATIONS

The proposed 1D model is shown in Figure 1. The atmosphere is stratified by gravity. The lower part of the atmosphere 1 is separated from the upper part 2 by a discontinuous decrease and increase in the equilibrium density and temperature, respectively. The discontinuity is located at $z = L$. Such a model could be a simple representation of the photosphere-chromosphere and chromosphere-corona environments. Slow magnetoacoustic waves are constrained to propagate upwards along the magnetic field. Assuming that the magnetic

pressure exceeds the plasma pressure inside a magnetic flux tube, we may set the tube speed equal to the sound speed. The sound waves, i.e., the p-modes are launched by a sinusoidal driver from the bottom of the atmosphere at $z = 0$. The vertical propagation of small amlitude waves is governed by the following set of linearised partial differential equations of continuity, momentum and energy:

$$\frac{\partial \rho}{\partial t} + \frac{\partial}{\partial z}(\rho_0 u) = 0, \tag{1}$$

$$\rho_0 \frac{\partial u}{\partial t} = -\frac{\partial p}{\partial z} - \rho_0 g, \tag{2}$$

$$\frac{\partial p}{\partial t} + \frac{\partial p_0}{\partial z} u = c^2(z) \left(\frac{\partial \rho}{\partial t} + \frac{\partial \rho_0}{\partial z} u \right), \tag{3}$$

where $c(z) = \sqrt{\gamma p_0(z)/\rho_0(z)}$ denotes the sound speed with γ the adiabatic index. The variations of equilibrium pressure p_0 and density ρ_0 are given by

$$p_0(z) = p_0(0) \exp\left(-\int_0^z \frac{dz}{\Lambda(z)} \right),$$

$$\rho_0(z) = \rho_0(0) \frac{\Lambda(z)}{\Lambda(z)} \exp\left(-\int_0^z \frac{dz}{\Lambda(z)} \right). \tag{4}$$

Here Λ is the pressure scale-height in the solar atmosphere determined by

$$\Lambda(z) = \frac{p_0(z)}{g\rho_0(z)} = \frac{c^2(z)}{\gamma g}. \tag{5}$$

The density and pressure perturbations ρ, p can be eliminated from Eqs (2)-(3). The result is a single second order partial differential equation for the velocity perturbation $u = u(z,t)$:

$$\frac{\partial^2 u}{\partial t^2} = c^2(z) \frac{\partial^2 u}{\partial z^2} + \frac{1}{\rho_0} \frac{\partial}{\partial z}(\rho_0 c^2) \frac{\partial u}{\partial z}. \tag{6}$$

By introducing a new variable

$$Q(z,t) = \sqrt{\frac{\rho_0(z) c^2(z)}{\rho_0(0) c^2(0)}} u(z,t), \tag{7}$$

Eq. (6) is reduced to the Klein-Gordon equation:

$$\mathcal{L}\, Q(z,t) = 0 \tag{8}$$

$$\text{where} \quad \mathcal{L} = \frac{\partial^2}{\partial t^2} - c^2(z) \frac{\partial^2}{\partial z^2} + \Omega^2(z) \tag{9}$$

is the Klein-Gordon operator and $\Omega(z) = c(z)/(2\Lambda(z))$ is the acoustic cutoff frequency. Eq. (8) has been applied to the study of wave propagation in an isothermal atmosphere. An excellent review is presented by Roberts (2004). In the present work, we apply the Klein-Gordon equation to the study of waves in non-isothermal media. This means that the coefficients of the operator (8) are functions of z. Eq. (8) is supplied with the boundary condition

$$\lim_{z \to 0} Q(z,t) = I(\omega) \cos(\omega t), \tag{10}$$

where $I = I(\omega)$ is the frequency dependent amplitude of the driver.

3. RESULTS AND DISCUSSION

For simplicity, we assume that Q is a complex variable. The boundary condition (10) is replaced with

$$\lim_{z \to 0} Q(z,t) = I(\omega) e^{-i\omega t}. \tag{11}$$

An equation of energy can be derived by substituting the operator (9) into the expression

$$\frac{\partial Q^*(z,t)}{\partial t} \mathcal{L} Q(z,t) + \frac{\partial Q(z,t)}{\partial t} \mathcal{L} Q^*(z,t),$$

where $*$ denotes complex conjugation. The result is

$$\frac{\partial W}{\partial t} = -\frac{\partial \mathcal{S}}{\partial z} \tag{12}$$

where

$$W = \frac{1}{2c^2} \left(\left| \frac{\partial Q}{\partial t} \right|^2 + c^2 \left| \frac{\partial Q}{\partial z} \right|^2 + \Omega^2 |Q|^2 \right) \tag{13}$$

is the mathematical wave energy density and

$$\mathcal{S} = -\Re \left(\frac{\partial Q}{\partial t} \frac{\partial Q^*}{\partial z} \right) \tag{14}$$

is the component of the mathematical wave energy flux in the z direction. The corresponding physical qunatities differ from the expressions (13) and (14) by scaling factors. Eq. (8) possesses steady state solutions of the form

$$Q(z,t) = A_n(\omega) e^{i(k_n(\omega) z - \omega t)} + B_n(\omega) e^{-i(k_n(\omega) z + \omega t)} \tag{15}$$

where the index $n = 1, 2$ represents the corresponding quantities in the lower $0 < z < L$ and upper $z > L$ regions. The wavenumber $k_n(\omega)$, $n = 1, 2$ is defined as follows:

$$k_n = \begin{cases} -i \dfrac{\sqrt{\Omega_n^2 - \omega^2}}{c_n}, & \omega < \Omega_n, \\ \dfrac{\sqrt{\omega^2 - \Omega_n^2}}{c_n}, & \omega > \Omega_n, \end{cases} \tag{16}$$

where c_n and Ω_n are the sound speed and cutoff frequency in the corresponding region. The coefficients A_n, B_n can be uniquely determined, if we impose certain physical requirements on the solution Q. The first condition follows from the requirement of continuity of the normal component of the Lagrangian displacement and the total equilibrium pressure at $z = L$. These conditions and Eq. (7) imply

$$Q(z,t)|_{z=L_+} = Q(z,t)|_{z=L+}, \tag{17}$$

i.e., the solution $Q(z,t)$ must be continuous accorss $z = L$. By integrating Eq. (6) with respect to z from $L - \varepsilon$ to $L + \varepsilon$ and taking the limit $\varepsilon \to 0$, we find that $\partial u/\partial z$

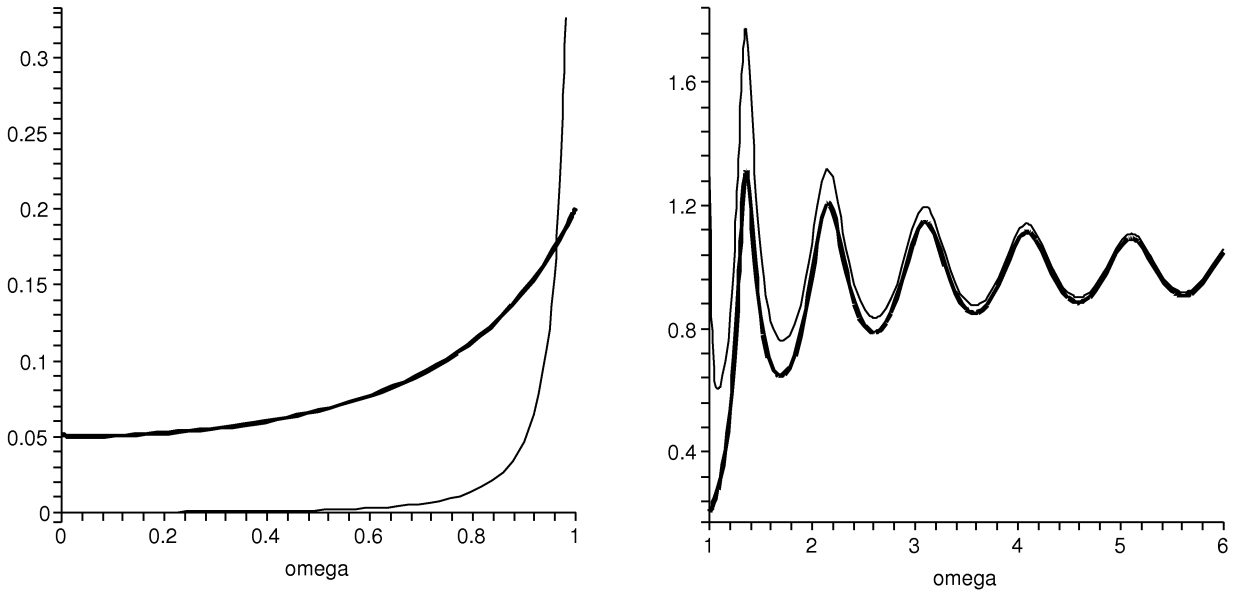

Figure 2. The scaled coefficients $|A_1(\omega)/I(\omega)|$ (thin line) and $|A_2(\omega)/I(\omega)|$ (thick line) as functions of frequency ω.

should be continuous accross $z = L$. Therefore, the second matching condition for $Q(z,t)$ has the form

$$\left(\frac{\partial Q}{\partial z} + \frac{1}{2\Lambda_1}Q\right)\Big|_{z=L-} = \left(\frac{\partial Q}{\partial z} + \frac{1}{2\Lambda_2}Q\right)\Big|_{z=L+}. \tag{18}$$

We also impose an outgoing wave condition at $z = L_+$. For $\omega > \Omega_2$ this implies $B_2 = 0$, consistent with the fact that the system contains no other sources of wave energy except at $z = 0$. Therefore, there is no energy flux from the upper region 2 into the lower region 1:

$$\mathcal{S}|_{z=L_+} = -\,\Re\left(\frac{\partial Q}{\partial t}\frac{\partial Q^*}{\partial z}\right)\Big|_{z=L_+} = k\omega(|A_2|^2) \geq 0. \tag{19}$$

On the other hand, for $\omega < \Omega_2$ we have to set $A_2 = 0$ in order to satisfy the requirement of finite wave energy density at $z = \infty$.

The resulting set of algebraic equations is solved for the coefficients A_n, B_n. We are mainly interested in the case $\omega > \Omega_2$, for which we obtain

$$\begin{aligned} A_2(\omega) &= \frac{I(\omega)k_1\exp(-ik_2L)}{e^{(ik_1L)} - \sin(k_1L)(ik_1 + ik_2 + \frac{1}{2\Lambda_2} - \frac{1}{2\Lambda_1})}, \\ A_1(\omega) &= \frac{I(\omega) - A_2(\omega)\exp[i(k_1+k_2)L]}{1-\exp(2ik_1L)}, \\ B_1(\omega) &= I(\omega) - A_1(\omega). \end{aligned} \tag{20}$$

The quantity $|A_2|$ determines the energy flux in the region above $z = L$ and represents the amplitude of the transmitted waves. We normalise length with respect to $2\Lambda_1$ and speed with respect to the sound speed c_1. This imples $\Omega_1 = 1$. The following parameter values are set: $T_2/T_1 = 100$, $L/\Lambda_1 = 6$. The quantities $|A_2/I|$ (thick line) and $|A_1/I|$ (thin line) are plotted in Figure 2 for

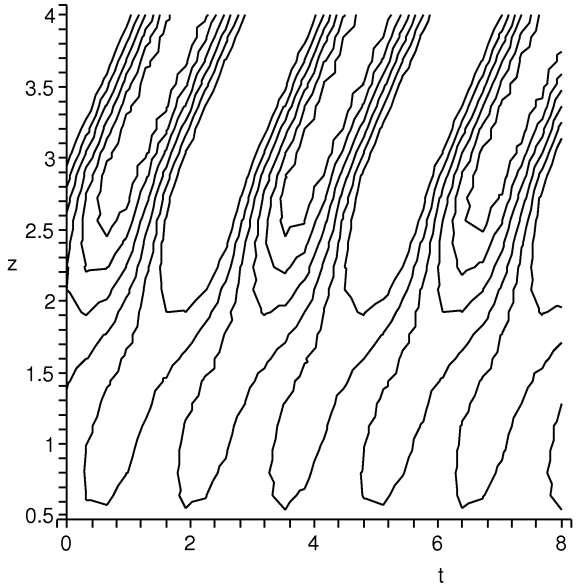

Figure 3. Time-distance plot for the scaled velocity $u(z,t)/I$. The driver frequency is $\omega = 2.1\Omega_1$ and the boundary is located at $L/(2\Lambda) = 3$.

$\omega < 1$ and $\omega > 1$. For $\omega < \Omega_1 = 1$ these coefficients are small meaning that very little energy is transmitted into the upper region. The scaled velocity Q is evanescent in the lower region as A_1 is small. This coefficient tends to infinity as the frequency approaches the cutoff value. However, the form of Eq. (15) implies that the solution remains finite for $0 < z < \infty$. When the frequency exceeds the cutoff value in the lower region, the absolute value of the coefficient A_2 increases and the amplitudes $|A_1|$, $|A_2|$ approach the amplitude of the original wave I as $\omega \to \infty$, i.e., the wave starts to propagate with no

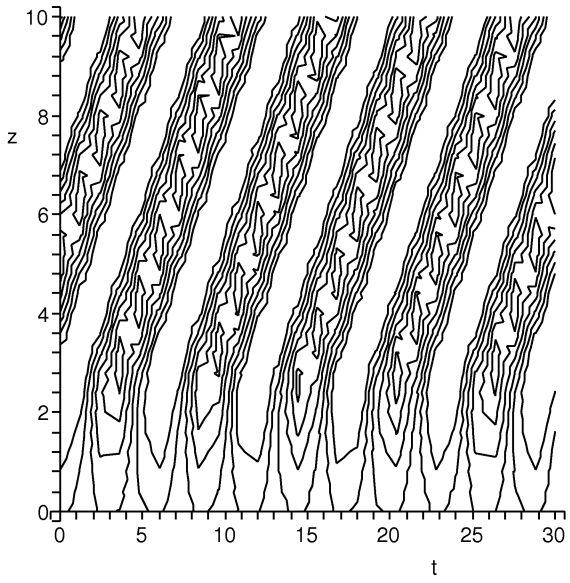

Figure 4. Time-distance plot for the scaled velocity $u(z,t)/I$. The driver frequency is $\omega = 1.1\Omega_1$ and the boundary is located at $L/(2\Lambda) = 3$.

reflection at the boundary $z = L$. A time-distance plot of the scaled velocity $u(z,t)/I$ is presented in Figure 3. The frequency exceeds the cutoff value ($\omega = 2.1\Omega$) and, therefore, the wave amplitude increases as it propagates towards the boundary at $L = 3$. An interesting feature occurs when the frequency of the prtopagating wave is close to the cutoff value in region 1. The time-distance plot for the case with $\omega = 1.1\Omega$ is plotted in Figure 4 It can be seen that the wave behaves like a standing wave in region 1 as opposed to region 2 where it propagates. A similar picture occurs when the model shown in Figure 1 is replaced with an empirical model with a VAL (Vernazza, Avrett, Loeser) atmosphere. The corresponding plot is shown in Figure 5. The agreement leads us to the conclusion that the simple model adopted in the present paper is a reasonable approximation to the real solar atmosphere. The slight discrepancy in the inclination of the curves in the upper regions is due to the increasing sound (propagation) speed in the empirical model as opposed to the constant sound speed c_2 in the present model. To explain the standing wave feature in the lower atmosphere, we set $k_1 = 0$ meaning that the frequency is close to the cutoff value. The solution $Q(z,t)$ takes the form

$$Q(z,t) = (A_1 + B_1 z)\exp(-i\omega t) \qquad (21)$$

Applying a sinmilar procedure as before, we find the following expressions for the coefficients A_n, B_n:

$$A_1 = I,\ B_1 = 0,$$
$$A_2 = \frac{I\exp(-ik_2 L)}{1 - ik_2 L + \frac{L}{2\Lambda_1} - \frac{L}{2\Lambda_2}} \qquad (22)$$

meaning that the real part of the solution has the form $Q = I(\omega)\cos(\omega t)$, i.e., it becomes a standing wave with a constant amplitude everywhere in the interval $0 < z < L$. This explains the feature seen in Figures 4 and 5.

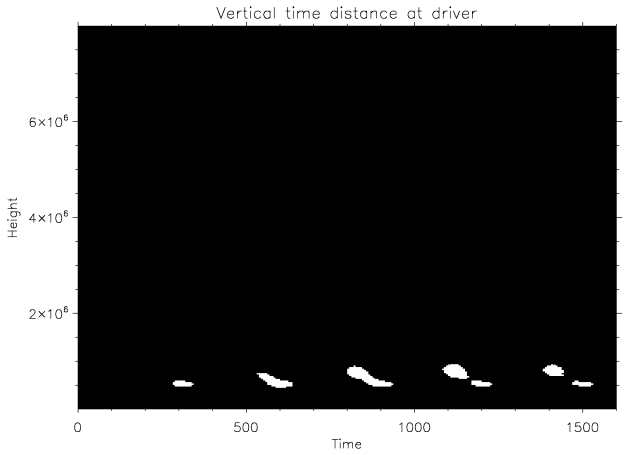

Figure 5. Time-distance plot for an empirical model with a VAL atmosphere. Height is measured in metres and time is measured in seconds. The driver period is 300 s. The cutoff heights are indicated with dotted lines. From about 1 Mm to 2 Mm the wave period is close to the cutoff period. The bounday L is represented by z=2 Mm.

ACKNOWLEDGMENTS

Y.T. is grateful to PPARC for financial support. R.E. acknowledges M. Kéray for patient encouragement and NSF, Hungary (OTKA, ref. no. TO43741). The simulations were run on the White Rose Grid (Iceberg node at Sheffield University).

REFERENCES

[1] Berghmans, D., & Clette, F. 1999, Sol. Phys., 186, 207

[2] De Moortel, I., Ireland, J., & Walsh, R.W. 2000, A&A, 355, L23

[3] De Pontieu, B., Erdélyi, R., & De Moortel, I. 2005, ApJ, 624, L61

[4] De Pontieu, B., Erdélyi, R., & De Wijn, A. G. 2003, ApJ, 595, L63

[5] De Pontieu, B., Erdélyi, R., & James, S. P. 2004, Nature, 430, 546

[6] Marsh, M.S., Walsh, R.W., 2006 ApJ, 643, 540

[7] Roberts, B., 2004, in proceedings of SOHO 13, ESA SP-547, 1

[9] Vernazza, J. E., Avrett, E. H., Loeser, R., 1981, APJS, 45, 635

[9] Chen, P. F., Priest, E. R., 2006, Springer Science, (in press)